

Local relaxation around Fe^{3+} in fluorides: Influence on electronic properties

J. A. Aramburu and J. I. Paredes

Departamento Ciencias de la Tierra y Física de la Materia Condensada, Facultad de Ciencias, Universidad de Cantabria, Avenida Los Castros s/n, 39005 Santander, Spain

M. T. Barriuso

Departamento de Física Moderna, Facultad de Ciencias, Universidad de Cantabria, Avenida Los Castros s/n, 39005 Santander, Spain

M. Moreno

Departamento Ciencias de la Tierra y Física de la Materia Condensada, Facultad de Ciencias, Universidad de Cantabria, Avenida Los Castros s/n, 39005 Santander, Spain

(Received 1 June 1999)

The local relaxation around Fe^{3+} impurities in different fluoride lattices has been explored by means of density-functional (DF) calculations on clusters including up to third neighbors of Fe^{3+} . For the same purpose the dependence of the isotropic superhyperfine constant, A_s , on the metal-ligand distance, R , has been studied for clusters of different size using the self-consistent charge extended Hückel and multiple-scattering $X\alpha$ methods as well. In all cases A_s is found to be proportional to R^{-n} , n lying between 6 and 7.5. Using this result the difference, ΔR_e , between the equilibrium distance for $\text{CsCdF}_3:\text{Fe}^{3+}$ and $\text{KMgF}_3:\text{Fe}^{3+}$ would be equal only to about 2.3 pm from the electron-nuclear double resonance (ENDOR) data reported for both systems. This figure, which has to be compared with the value $\Delta R_0 = 23$ pm corresponding to the perfect host lattice, is compatible with the R_e values derived from total-energy calculations. Although the value $\Delta R_e = 2.3$ pm is much smaller than $\Delta R_e = 7 \pm 1$ pm corresponding to Mn^{2+} in the same lattices, it is shown to be consistent with the $\omega(A_{1g})$ frequency for both kind of impurities. From the present results R_e changes caused by a hydrostatic pressure down to 0.05 pm can be detected through A_s variations measured by ENDOR. Moreover it is pointed out that good information about the actual impurity-ligand distance for transition-metal impurities in insulators can be obtained from DF calculations on clusters. Finally, the $10Dq$ value and its R dependence are shown to be strongly related to the small $3d-2s(F)$ hybridization in the antibonding e_g^* level which also determines A_s .

I. INTRODUCTION

The presence of transition-metal (TM) impurities in insulators gives rise to the appearance of interesting properties. A good characterization of the local structure around the impurity is a prerequisite for gaining a better insight into the microscopic origin of such properties. Although for a pure compound the measurement of interatomic distances can be carried out through standard x-ray or neutron-diffraction techniques, such techniques are, however, not useful in the case of diluted impurities.

In order to determine the actual equilibrium distance, R_e , between an impurity and the nearest-neighbor ligands, three different approaches have been used in the last years: (i) the extended x-ray-absorption fine-structure (EXAFS) technique;¹⁻⁵ (ii) the analysis of electron paramagnetic resonance (EPR) and optical parameters⁶⁻¹² sensitive to variations of the metal-ligand distance, R ; (iii) realistic quantum-mechanical calculations on clusters centered around the impurity.¹³⁻¹⁸

Although the EXAFS technique can be applied to a number of different kinds of impurities, it often requires impurity concentrations higher than 1000 ppm. At the same time the uncertainty on the obtained R_e value is higher than ± 1 pm and thus R_e changes induced by thermal expansion effects or hydrostatic pressures smaller than about 5 GPa can hardly be detected through such a technique. This situation can, how-

ever, be substantially improved looking at some EPR or optical parameters such as the isotropic superhyperfine (shf) constant,^{7,11} A_s , or the cubic field splitting parameter,^{8,9,11} $10Dq$. Also the zero-phonon line energy of crystal-field transitions which are $10Dq$ dependent has been employed for this purpose.¹⁰

In the realm of TM impurities in insulators a good structural characterization has been accomplished for substitutional Mn^{2+} impurities in fluoroperovskites. Along this series the $\text{Mn}^{2+}-\text{F}^-$ distance was determined through the analysis of experimental A_s and $10Dq$ parameters^{7,8} and also by EXAFS¹⁹ in the case of $\text{KZnF}_3:\text{Mn}^{2+}$ and $\text{RbCdF}_3:\text{Mn}^{2+}$. For each compound of the series these methods lead to the same R_e value within the experimental uncertainties. Using the A_s constant measured by means of the electron-nuclear double resonance (ENDOR) technique R_e changes down to 0.03 pm can be detected in these systems.⁷ Although Fe^{3+} is isoelectronic to Mn^{2+} fewer efforts have been devoted, however, towards achieving a structural characterization of Fe^{3+} impurities in halides. This partially comes from the usual absence of luminescence for Fe^{3+} impurities in octahedral coordination^{20,21} which can act as killers of the luminescence due to other sources.²² This circumstance prevents the observation of excitation spectra and thus the measurement of $10Dq$, in the case of diluted impurities.

Despite this fact the shf interaction has often been de-

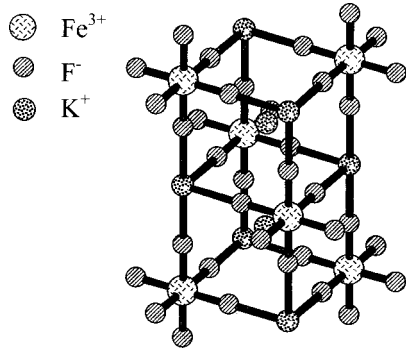


FIG. 1. Picture of the elpasolite K_3FeF_6 lattice following Ref. 35.

tected through EPR for Fe^{3+} in fluoride lattices.^{23–31} Moreover, precise measurements of the shf tensor have been carried out by ENDOR in the case of *cubic centers* formed in some Fe^{3+} -doped fluoroperovskites.^{25–29} Therefore, it is crucial to investigate whether for Fe^{3+} in fluorides some insight about the true distance between a Fe^{3+} impurity and its nearest neighbors can also be derived from the analysis of the experimental shf tensor. Hartree-Fock calculations on isolated FeF_6^{3-} units performed³² *only* at $R=1.90 \text{ \AA}$ and $R=2.00 \text{ \AA}$ suggested a strong R dependence of A_s .

The present work is devoted to exploring the local relaxation around Fe^{3+} impurities in cubic fluorides. For achieving this goal, theoretical calculations of the equilibrium metal-ligand distance, R_e , using clusters of *different sizes* centered around the impurity, have been performed in a first step. Calculations have been carried out in the density-functional theory (DFT) framework using the Amsterdam density functional (ADF) code.^{33,34} Good results on equilibrium distances of TM cations in insulating materials have recently been obtained using DFT. In the case of Cr^{3+} -doped fluoroelpasolites, the calculated R_e values¹⁸ using clusters including up to third neighbors are coincidental with experimental ones within $\pm 1.5\%$.

For the present case, K_3FeF_6 and $LiF:Fe^{3+}$ systems have first been explored. Although K_3FeF_6 is in fact a Fe^{3+} compound (Fig. 1), where R_e is thus well determined, two close Fe^{3+} ions lie, however, far apart (the distance between them being 6.07 \AA) and *do not share* any common ligand. In the present calculations the electrostatic potential, V_R , due to the rest of the lattice *not included* in the cluster has been considered. Particular attention has been paid to explore the dependence of the computed R value on the cluster size and also the *nonflatness* of V_R inside the cluster. As recently found for Cr^{3+} impurities, the R_e values computed using clusters including third neighbors are found to be in the range of experimental Fe^{3+} - F^- distances^{35–39} for some representative compounds.

In a second step we have tried to correlate the experimental value of A_s for FeF_6^{3-} in different cubic lattices with the actual value of R_e . As is known through Sugano and Shulman,⁴⁰ the electronic properties due to a *substitutional* TM impurity, M , in an insulator can be understood to a good extent considering only the MX_n complex (formed with the nearest anions X) at the *right* equilibrium distance. This important idea means that variations undergone by EPR or optical parameters due to a complex in a series of host lattices

TABLE I. Experimental values of the isotropic shf constant A_s (in MHz) corresponding to Fe^{3+} and Mn^{2+} impurities embedded in different cubic fluoride lattices and an aqueous solution with NH_4F . In all cases the impurities are surrounded by six F^- ions displaying octahedral symmetry. Values for $KMF_3:Fe^{3+}$ ($M=Zn, Mg$) and $ACdF_3:Fe^{3+}$ ($A=Rb;Cs$) have been measured through ENDOR. The rest of the values have been obtained by EPR at room temperature. For comparison, the A_s value for $ACdF_3:Fe^{3+}$ at room temperature is $A_s=65.5 \pm 1.2 \text{ MHz}$ (Ref. 30). References on experimental work on Mn^{2+} in fluorides can be found in Ref. 7. The lattice constant, a (in \AA), of the host lattice is also given.

System	a	A_s	Ref.
$K_2NaGaF_6:Fe^{3+}$	8.24	67.3 ± 1.4	23
$Rb_2KGaF_6:Fe^{3+}$	8.79	62 ± 2.8	24
$KMgF_3:Fe^{3+}$	3.988	71.23 ± 0.06	25
$KZnF_3:Fe^{3+}$	4.054	70.3 ± 0.3	26
$KCdF_3:Fe^{3+}$	4.334	68.1 ± 1.4	27
$RbCdF_3:Fe^{3+}$	4.400	66.1 ± 0.3	28
$CsCdF_3:Fe^{3+}$	4.464	65.98 ± 0.02	29
$NH_4F(aq):Fe^{3+}$		64.8 ± 1.5	31
$KMgF_3:Mn^{2+}$	3.998	54.3 ± 2.1	7
$CsCdF_3:Mn^{2+}$	4.464	42.6 ± 0.9	7
$CsCaF_3:Mn^{2+}$	4.524	39.6 ± 0.9	7

with the *same* structure would reflect the change of the metal-ligand distance along the series. This behavior has proved true for cations such as Mn^{2+} , Cr^{3+} , Ni^{2+} , or Ni^+ in different halide lattices^{7–11,41} or Cr^{4+} in oxides.⁴²

For greater confidence on the reliability of theoretical predictions about the R dependence of A_s , multiple-scattering $X\alpha$ (MS- $X\alpha$) and self-consistent charge extended Hückel (SCCEH) methods have been used together with the ADF code. The first two methods give reasonable results for the electronic properties of TM impurities (when computed around the experimental equilibrium distance), but not on total energies, equilibrium distances, or vibrational frequencies.

As for the interpretation of experimental A_s values for Fe^{3+} and Mn^{2+} in some fluoride lattices (collected in Table I) a point deserves special attention. In the case of Mn^{2+} the difference between the highest and lowest A_s value is equal to 16 MHz while it is practically half in the case of Fe^{3+} . More precisely, the difference between the A_s value measured^{25,29} by ENDOR in $KMgF_3:Fe^{3+}$ and $CsCdF_3:Fe^{3+}$ is well established as equal only to $5.25 \pm 0.08 \text{ MHz}$. For being sure that such a difference actually reflects a different R_e value in both systems, the R_e value for $KMgF_3:Fe^{3+}$ and $RbCdF_3:Fe^{3+}$ has also been calculated by means of the ADF code. In a further step we have tried to explain why such a difference is much smaller than the corresponding figure ($12 \pm 3 \text{ MHz}$) measured⁷ by EPR in the case of Mn^{2+} .

II. THEORETICAL

Density-functional calculations of this work have been performed using the ADF code.^{33,34} Triple zeta basis functions of quality IV, which are implemented in the ADF code, are employed. For Fe^{3+} , electrons up to the $3p$ shell are kept

TABLE II. Expression of $2s$, $3s$, and $4s$ normalized Kohn–Sham orbitals (in a.u.) corresponding to the free fluorine atom as a combination of one $1s$ and three $2s$ Slater-type orbitals. Note that the nonzero density at the nucleus depends only on the contribution associated with the $1s$ Slater-type orbital. The values of the N_i coefficients ($i = 1, \dots, 4$) are the following: $N_1 = 48.08$, $N_2 = 0.553$, $N_3 = 605$ and $N_4 = 21.82$.

$\sqrt{4\pi} s_2^0\rangle = (0.275N_1e^{-8.33r} + 0.022N_2re^{-0.74r} - 0.551N_3re^{-1.94r} - 0.538N_4re^{-3.24r})$
$\sqrt{4\pi} s_3^0\rangle = (-0.065N_1e^{-8.33r} - 1.202N_2re^{-0.74r} + 0.528N_3re^{-1.94r} + 0.029N_4re^{-3.24r})$
$\sqrt{4\pi} s_4^0\rangle = (-0.43N_1e^{-8.33r} + 0.697N_2re^{-0.74r} - 2.515N_3re^{-1.94r} + 2.312N_4re^{-3.24r})$

frozen so as the $1s$ electrons of F⁻. The local-density approximation (LDA) exchange-correlation energy was computed according to Vosko, Wilk, and Nusair's parametrization⁴³ of electron-gas data. In the case of generalized gradient approximation (GGA) calculations, we opted for the Becke-Perdew functional,⁴⁴ which uses Becke's gradient correction to the local expression of the exchange energy and Perdew's gradient correction to the local expression of the correlation energy.

In the studied clusters only the impurity-ligand distance has been taken as variable while second and third neighbors are fixed at their host-lattice positions. This approximation is more valid as far as the absolute value of the displacement $u = (R_e - R_0)$ undergone by the ligands decreases. Here R_0 means the distance corresponding to the perfect host lattice.

Because of the role played by the isotropic shf constant in the present analysis, let us first briefly discuss its meaning in a traditional molecular orbital (MO) picture. Later, the way of calculating the shf constant A_s by means of the ADF code is explained in some detail.

The shf constant A_s in complexes such as FeF₆³⁻ or MnF₆⁴⁻ comes essentially from the two unpaired electrons in the e_g^* level where the $3d-2s(F)$ hybridization is symmetry allowed.^{27,45,7} In a MO description the $|e_g^*; j\rangle$ wave function ($j = 3z^2 - r^2; x^2 - y^2$) is briefly written as

$$|e_g^*; j\rangle = N_e \{ |d; j\rangle - \lambda_{p\sigma} |\chi_{p\sigma}; j\rangle - \lambda_s |\chi_s; j\rangle \}, \quad (1)$$

where, for instance, $|\chi_s; j\rangle$ means a suitable linear combination of atomic orbitals (LCAO) of the six atomic $2s(F)$ orbitals. The expression of A_s in terms of N_e and λ_s parameters is⁷

$$A_s = \frac{1}{2S} f_s A_s^0, \quad (2)$$

$$f_s = \frac{1}{3} (N_e \lambda_s)^2.$$

In Eq. (2), f_s is the spin density transferred onto an atomic $2s(F)$ orbital and $A_s^0 = 44\,964$ MHz corresponds to a single $2s(F)$ electron. The factor $2S = 5$ for the present cases underlines that *only one* among the five unpaired electrons can be on the $2s$ orbitals of two F⁻ ions on the OZ axis. For purposes of comparison, the R dependence of the spin density onto the $2p(F)$ orbital, $f_{\sigma} = (N_e \lambda_{p\sigma})^2 / 3$, will also be briefly discussed.

In DFT calculations the right density of the ground state is written in terms of the occupied Kohn–Sham (KS) orbitals denoted as $|\phi(k)\rangle$. These orbitals are, however, the right wave functions of the *associated* system involving *noninter-*

acting electrons.⁴⁶ In the ADF code the normalized KS orbital $|\phi(3z^2 - r^2)\rangle$ is briefly written as

$$|\phi(e_g^*; 3z^2 - r^2)\rangle = |\phi(3d)\rangle - |\phi(2p\sigma)\rangle - |\sigma(2s)\rangle. \quad (3)$$

As to the $2s$ admixture, $|\phi(2s)\rangle$, using triple zeta basis, it is expressed as follows:

$$|\phi(2s)\rangle = \sum_{i=2}^4 c_i |\phi_i^0(s)\rangle,$$

$$|\phi_i^0(s)\rangle = \frac{1}{\sqrt{12}} \{ 2|s_i^0(5)\rangle + 2|s_i^0(6)\rangle - |s_i^0(1)\rangle - |s_i^0(2)\rangle - |s_i^0(3)\rangle - |s_i^0(4)\rangle \}. \quad (4)$$

Here $|s_i^0(l)\rangle$ ($i = 2, 3, 4$) denote the $2s$, $3s$, and $4s$ KS orbitals of free F⁰ atom corresponding to the l -number ligand ($l = 1, 2, \dots, 6$). Ligand numbers 5 and 6 lie on the OZ axis of the FeF₆³⁻ complex. The expressions of normalized $|s_i^0(l)\rangle$ orbitals are given in Table II. Therefore the values of f_s and A_s in the spin restricted DFT framework are

$$f_s = \frac{1}{3} \sum_{i=2}^4 c_i^2, \quad (5)$$

$$A_s(\text{MHz}) = (8\pi/3) 2\beta\beta_N g_N \|\phi(2s)\|_{r=0}^2 = 51504 \left(\sum_{i=2}^4 c_i \alpha_i \right)^2,$$

where β , β_N , and g_N are, respectively, the Bohr magneton, the nuclear magneton, and the gyromagnetic ratio of ¹⁹F. The values $\alpha_2 = 0.275$, $\alpha_3 = -0.065$, $\alpha_4 = -0.43$ are taken from $1s$ -type Slater orbitals in Table II. One expects *a priori* that c_2 should dominate over c_3 and c_4 , A_s being then proportional to f_s . This condition is verified by all the calculations shown in this work.

Details about MS-X α and SCCEH calculations can be found elsewhere.⁴⁷

III. RESULTS

A. Equilibrium distances for Fe³⁺ in LiF and K₃FeF₆

Values of the computed Fe³⁺-F⁻ distance in K₃FeF₆ using clusters of different size are shown in Table III, where the R_e value calculated for the FeF₆³⁻ complex *in vacuo* is also given for comparison. Similar results on the Fe³⁺ impurity embedded in LiF are displayed in Table IV. In all cases the R_e values derived using both LDA and GGA functionals are reported. As it can be seen the *main trends* reached through both functionals are the same.

TABLE III. ADF results for the equilibrium $\text{Fe}^{3+}\text{-F}^-$ distance, R_e (in Å), in different clusters simulating the K_3FeF_6 system and using both LDA and GGA functionals. In some cases the electrostatic potential due to the rest of the lattice, V_R^{el} , and the Born-Mayer interaction between F^- ligands and nearest K^+ ions, V_{BM} , were considered. In the calculations only the position of F^- ligands is allowed to vary, the rest of the ions being kept fixed in the perfect lattice positions.

Cluster	Calculation	LDA	GGA
FeF_6^{3-}	<i>In vacuo</i>	2.03	2.10
FeF_6^{3-}	V_R^{el}	2.00	2.07
FeF_6^{3-}	$V_R^{\text{el}} + V_{\text{BM}}$	1.87	1.84
$\text{FeF}_6\text{K}_8\text{K}_6^{11+}$	<i>In vacuo</i>	1.90	1.92
$\text{FeF}_6\text{K}_8\text{K}_6^{11+}$	V_R^{el}	1.90	1.92

The equilibrium distance computed for the FeF_6^{3-} unit alone is not far from experimental values measured for *pure* compounds containing such a complex. It can be seen in Table IV that, for compounds such as K_2NaFeF_6 or FeF_3 , R_e is close to 1.92 Å while the older measurements³⁵ for K_3FeF_6 gave $R_e = 1.85$ Å. For the FeF_6^{3-} complex *in vacuo* the computed R_e value is equal to $R_e = 2.02$ Å using the LDA functional while a slightly higher value ($R_e = 2.10$ Å) is obtained through the nonlocal GGA functional.

When the complex is allowed to feel *only* the electrostatic potential due to the rest of the lattice, V_R^{el} , the equilibrium distance is reduced. This reduction is more important for $\text{LiF}:\text{Fe}^{3+}$ than for K_3FeF_6 . These results can qualitatively be understood looking at the form of the electrostatic energy, $U_R^{\text{el}} = -eV_R^{\text{el}}$, displayed in Fig. 2. In the case of K_3FeF_6 , U_R^{el} at the ligand position is 0.3 eV higher than at the Fe^{3+} position which implies a force on ligands *towards* the central ion. In the case of $\text{LiF}:\text{Fe}^{3+}$ the latter figure becomes equal to 1.2 eV, thus inducing a stronger reduction of R_e than for the FeF_6^{3-} complex subjected to the electrostatic potential of the K_3FeF_6 lattice.

The behavior of U_R^{el} displayed in Fig. 2 can easily be understood in lattices where ligands occupy a centrosymmetric position. In general the total electrostatic potential, V_T^{el} , due to all other ions around a lattice point in the perfect host

TABLE IV. Calculated impurity ligand equilibrium distances, R_e (in Å), for $\text{LiF}:\text{Fe}^{3+}$ using clusters of different size. In some cases the influence of V_R^{el} and V_{BM} is also shown. Only the situation corresponding to a remote charge compensation, not affecting the local O_h symmetry, has been computed. In the calculation, only the position of the ligands is allowed to vary, the rest of the ions being kept fixed. As done in Table II, the R_e values derived through both LDA and GGA functionals are given.

Cluster	Calculation	LDA	GGA
FeF_6^{3-}	<i>In vacuo</i>	2.03	2.10
FeF_6^{3-}	V_R^{el}	1.93	1.97
FeF_6^{3-}	$V_R^{\text{el}} + V_{\text{BM}}$	1.89	1.93
$\text{FeF}_6\text{Li}_{12}\text{F}_8^{1+}$	<i>In vacuo</i>	1.95	2.00
$\text{FeF}_6\text{Li}_{12}\text{F}_8^{1+}$	V_R^{el}	1.94	1.99
$\text{FeF}_6\text{Li}_{12}\text{F}_8\text{Li}_6^{7+}$	V_R^{el}	1.93	1.95

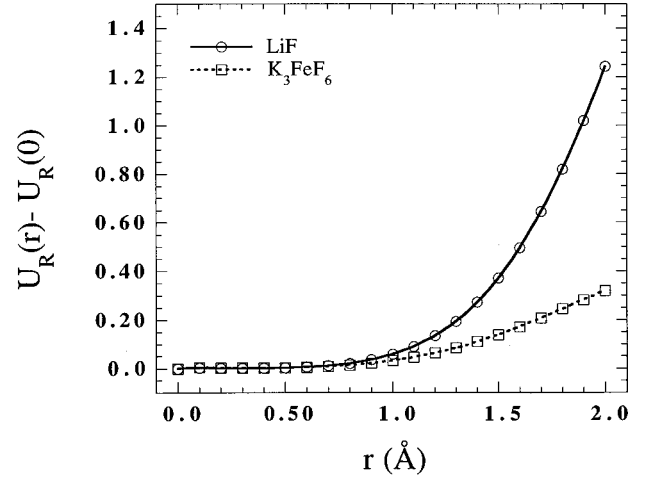


FIG. 2. Plot of the electrostatic energy, U_R , for an electron in the FeF_6^{3-} cluster due to the electrostatic potential of the rest of the lattice as a function of the distance, r , between the electron and the iron nucleus. In the figure the r dependence of U_R is shown for two different host lattices when the electron is moved along $\langle 100 \rangle$ directions. The value of U_R at the iron position is equal to -30.5 eV for LiF and to -14.8 eV for the elpasolite K_3FeF_6 .

lattice, can be written as $V_T^{\text{el}} = V_C^{\text{el}} + V_R^{\text{el}}$. Here V_C^{el} denotes the contribution due to the other ions *in* the M^*X_n complex corresponding to the host lattice. M^* is thus the host-lattice cation. If the ligand is in a centrosymmetric position, then $\partial V_R^{\text{el}}/\partial \mathbf{R}_L = -\partial V_C^{\text{el}}/\partial \mathbf{R}_L$, where \mathbf{R}_L means the ligand position vector. Therefore, for a LiF lattice in the vicinity of the ligand at $(R_0, 0, 0)$, $\partial U_R^{\text{el}}/\partial X = 0.66e^2/R_0^2$, where R_0 is the $\text{Li}^+\text{-F}^-$ distance. This simple formula leads to a value close to 2 eV/Å in agreement with Fig. 2. This procedure, which cannot be applied to an elpasolite lattice, indicates that $\partial U_R^{\text{el}}/\partial X$ is negative at a ligand position for a cubic perovskite such as KMgF_3 .

Going beyond the description of a FeF_6^{3-} complex feeling *only* the electrostatic potential of the rest of the lattice the full interaction between the six F^- ions of the FeF_6^{3-} complex and further neighbors has also been incorporated. In the first step, the interaction with second neighbors, modeled by means of empirical Born-Mayer potentials (V_{BM}) has been included. Such an interaction, as expected, leads to a slight diminution of R_e for both systems. It is worth noting that after the inclusion of V_R and V_{BM} , R_e is slightly smaller for K_3FeF_6 than for $\text{LiF}:\text{Fe}^{3+}$.

Trying to improve the reliability of the present results ADF calculations on bigger clusters have been carried out in a second step. The results, collected in Tables III and IV, indicate (i) the best R_e value reached through the present calculations for K_3FeF_6 lies in the 1.90–1.92 Å range; (ii) despite the differences between the K_3FeF_6 and LiF lattices, the final $\text{Fe}^{3+}\text{-F}^-$ distance in LiF turns out to be *only* about 0.03 Å higher than in the former case. Moreover, this result indicates the existence of an inwards relaxation of about 8 pm accompanying the substitution of Li^+ by Fe^{3+} in LiF. Although this trend is according to the ionic radius of Fe^{3+} and Li^+ , there is no supplementary evidence of it. Additional experimental information about the local relaxation exists for Fe^{3+} -doped fluoroperovskites which is analyzed in Secs. III B and III C.

TABLE V. Representative values of the experimental average $\text{Fe}^{3+}-\text{F}^-$ distance, R_e (in \AA), measured for some pure compounds containing perfect or distorted FeF_6^{3-} units. Additional data can be found in Ref. 36.

Compound	R_e	Ref.
FeF_3	1.922	36
K_2NaFeF_6	1.910	39
$\text{HgFeF}_5 \cdot 2\text{H}_2\text{O}$	1.941	37
K_2FeF_5	1.937	38
KFeF_4	1.916	36
K_3FeF_6	1.850	35
$\text{Cs}_2\text{NaFeF}_6$	1.922	36

It is worth noting that the experimental R_e value, measured for a number of pure compounds involving the FeF_6^{3-} complex (Table V), lies in the 1.90–1.95 \AA range. The only exception to this behavior comes from the data³⁶ on the K_3FeF_6 elpasolite measured in the fifties. In a subsequent study it was found^{48,49} that the crystal structure of K_3FeF_6 exhibits a slight distortion from cubic symmetry, the average R_e value being equal to 1.90 \AA . Therefore, the R_e values calculated in Tables III and IV by means of the biggest clusters are comparable to experimental figures collected in Table V. Such a comparison also indicates that the error involved in the calculated R_e values would be around $\pm 1.5\%$. This result is thus similar to that recently obtained for Cr^{3+} in fluoroelpasolites.¹⁸

In order to have a supplementary checking about the reliability of the present ADF calculations the total energy as a function of R has been computed for the 21-atom $\text{FeF}_6\text{K}_8\text{K}_6^{11+}$ cluster. From it a value $\hbar\omega(A_{1g}) = 590 \text{ cm}^{-1}$ has been derived from the symmetric mode of the FeF_6^{3-} unit (Fig. 3). It is worth noting that the experimental $\hbar\omega(A_{1g})$ value for MF_6^{3-} complexes (where M is a trivalent $3d$ ion) lies⁵⁰ between 500 and 600 cm^{-1} . More precisely, for the Rb_2KFeF_6 compound⁵¹ $\hbar\omega(A_{1g})$ is equal to 530 cm^{-1} while a value $\hbar\omega(A_{1g}) = 538 \text{ cm}^{-1}$ has been reported⁵² for $(\text{NH}_4)_3\text{FeF}_6$.

B. Dependence of the isotropic superhyperfine constant A_s on R

As pointed out in Sec. II the transferred spin density, f_s , is directly related to the isotropic shf constant, A_s , which for Fe^{3+} in fluorides lies around 67 MHz (Table I). In Fig. 4 the R dependence of f_s calculated using different methods for the simple FeF_6^{3-} unit is shown. All methods lead to f_s values in the range 1.2–1.6% for $R = 1.9 \text{\AA}$, as well as to a strong R dependence of f_s . In fact, setting around $R_e = 1.91 \text{\AA}$ the R dependence of f_s as

$$f_s = KR^{-n_s}, \quad (6)$$

all the calculated n_s values are close to 6.5. In Figs. 5 and 6 the results for f_s and f_σ reached in the case of a 21-atom cluster simulating Fe^{3+} in K_3FeF_6 are shown. Again, all calculations lead to a strong sensitivity of f_s to R variations, the exponent n_s lying between 6 and 7.5. It is worth noting, however, that in this case, the MS-X α and SCCEF values of

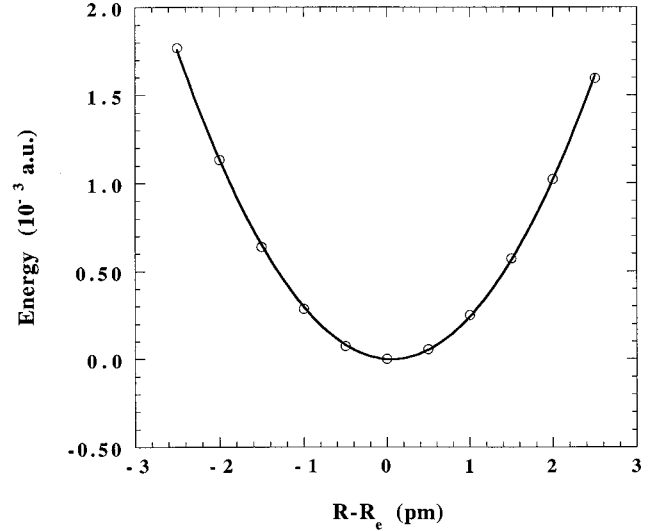


FIG. 3. Ground-state energy as a function of the $\text{Fe}^{3+}-\text{F}^-$ distance (R) calculated for the $\text{FeF}_6\text{K}_8\text{K}_6^{11+}$ cluster by means of the ADF method and the LDA functional. Here, R_e means the equilibrium distance at zero pressure which is found to be equal to 1.90 \AA . The value of the computed frequency $\omega(A_{1g})$ is equal to 590 cm^{-1} . The zero of energy is taken at the equilibrium position. Only the ligand position is considered as variable.

f_s obtained at $R = 1.9 \text{\AA}$ are closer to the experimental ones than the figures derived from ADF calculations. As to the A_s parameter itself the present calculations lead to values which are somewhat higher than experimental ones. For instance, restricted ADF calculations carried out on a $\text{FeF}_6\text{K}_8\text{K}_6^{11+}$ cluster give $A_s = 125.5 \text{ MHz}$ at $R = 1.91 \text{\AA}$, while $A_s = 111.6 \text{ MHz}$ at $R = 1.95 \text{\AA}$. This result thus stresses that a

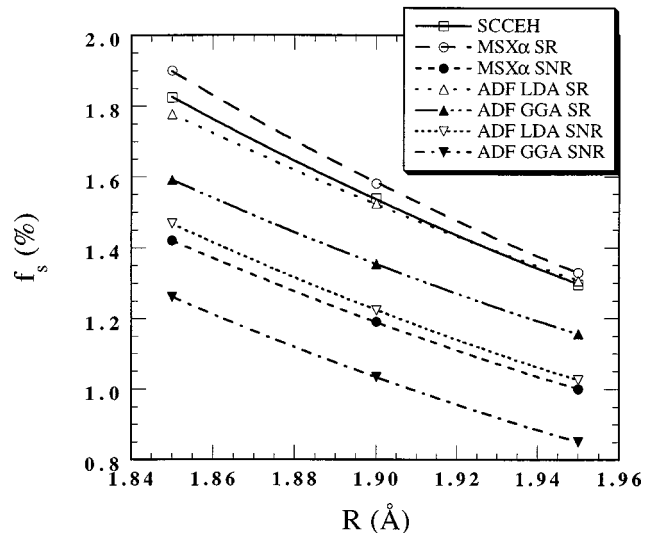


FIG. 4. Dependence of the transferred spin density, f_s (in %) on the metal-ligand distance, R , calculated on a simple FeF_6^{3-} cluster by different methods. LDA and GGA mean local-density and generalized gradient approximation, respectively, while SR (SNR) denotes a spin restricted (spin unrestricted) calculation. In MSX α and SCCEH calculations a Watson sphere has been used while in all ADF calculations the FeF_6^{3-} unit is subjected to the influence of the electrostatic potential of a LiF lattice. Note that the relative variations found by these calculations are very similar.

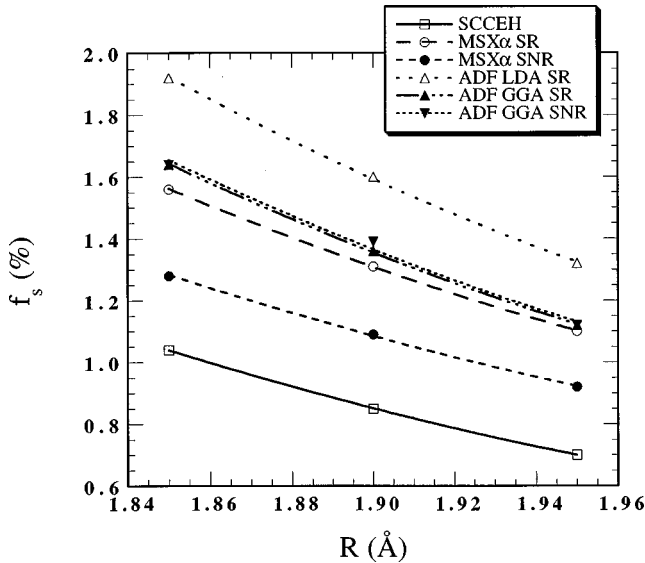


FIG. 5. Dependence of the transferred spin density, f_s (in %) on the metal-ligand distance, R , calculated on a $\text{FeF}_6\text{K}_8\text{K}_6^{11+}$ cluster simulating a Fe^{3+} ion in the K_3FeF_6 lattice. The electrostatic potential due to the rest of ions in the K_3FeF_6 lattice has been taken into account. The meaning of symbols is the same as that in Fig. 4. All calculations lead to a strong dependence of f_s upon R .

calculation which reproduces quite well the experimental R_e value is, however, unable to reproduce exactly *fine details* of the ground-state density such as f_s . As found for other TM cations, f_σ is much higher than f_s but is nearly independent on the metal-ligand distance, R . So setting f_σ in the vicinity of $R = 1.91 \text{ \AA}$ as

$$f_\sigma = CR^{-n_\sigma}, \quad (7)$$

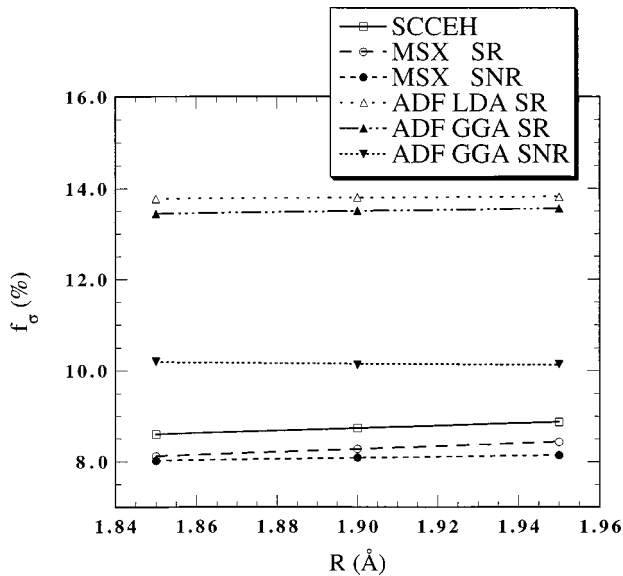


FIG. 6. Dependence of the transferred spin density, f_σ (in %) on the metal-ligand distance, R , calculated on a $\text{FeF}_6\text{K}_8\text{K}_6^{11+}$ cluster simulating a Fe^{3+} ion in the K_3FeF_6 lattice. The electrostatic potential due to the rest of ions in the K_3FeF_6 lattice has been taken into account. The meaning of symbols is the same as that in Fig. 4. All the calculations indicate that in a first approximation f_σ is independent of R .

all the n_σ values derived from Fig. 6 are comprised between 1.3 and -1.3 obtained in ADF and MS- $X\alpha$ calculations, respectively.

This remarkable difference between the sensitivity displayed by f_σ and f_s to changes of R has recently been explained.^{47,53} In essence, in a simple MO framework f_σ not only depends on the square of the group overlap integral $S_\sigma = \langle d; j | \chi_{p\sigma}; j \rangle$, but also on $\{E(3d) - E(2p)\}^{-2}$, where $E(3d) - E(2p)$ means an average metal to ligand charge-transfer excitation. Upon increasing R the increase experienced by the overlap integral S_σ is compensated by the increase undergone by the $E(3d)$ energy. This behavior leads to an increase of charge-transfer excitations when R is reduced, as has recently been discussed.¹⁸ By contrast, the R dependence of f_s is essentially that followed by $S_s^2 = |\langle d; j | \chi_s; j \rangle|^2$. The latter fact comes from the great difference $E(2p) - E(2s) = 23 \text{ eV}$ for free F^- ion making that the relative variations undergone by the $E(3d) - E(2s)$ quantity due to R changes are negligible. Further discussion on this relevant point can be found in Ref. 51.

When the properties associated with an impurity are calculated by means of finite clusters the results can oscillate with the cluster size. This fact was already noticed by Messmer and Watkins.⁵⁴ In the present case quantities such as f_σ or N_e^2 depend only slightly upon the cluster size. It has been verified that in a SCCEH calculation on passing from a 7-atom TM cluster to an 81-atom one f_σ and N_e^2 experience variations of about 20 and 2%, respectively. By contrast, the calculated values of f_s are more dependent on cluster size mainly because of the smallness of this parameter (Figs. 4 and 5). In fact, when the cluster involves a total of 21 or 81 atoms, the electronic density in the e_g^* orbital lying outside the FeF_6^{3-} unit is found to be only around 3%. However, this figure is quite comparable to the total density on $2s(F)$ ligand orbitals.

Despite the differences of the f_s value, obtained at a given distance, Figs. 4 and 5 reveal that *all* exponents n_s calculated by *different* methods and on clusters of different size are rather *similar*, lying between 6 and 7.5. This result thus do support the use of A_s for measuring R_e variations induced by hydrostatic pressures on a given system containing FeF_6^{3-} units. At the same time it can also be employed for exploring the R_e variations undergone by FeF_6^{3-} units placed in a series of similar lattices.

C. Equilibrium distance values for Fe^{3+} doped fluoroperovskites

Assuming the results of the Sec. III B, an A_s variation of $\pm 4 \text{ MHz}$ around a central value of 67 MHz should be ascribed to R_e changes lying about between -2 and $+2 \text{ pm}$. Therefore, in a first view, the A_s values collected in Table I would indicate that the corresponding R_e values lie in a range of about 5 pm. This conclusion is thus compatible with results of Table V and Sec. III A.

To proceed further in the analysis let us now consider only the case of cubic Fe^{3+} centers formed in fluoroperovskites where A_s has accurately been measured by ENDOR. In these similar lattices A_s goes^{25,26,28,29} from $71.23 \pm 0.06 \text{ MHz}$ for $\text{KMgF}_3:\text{Fe}^{3+}$ to $65.98 \pm 0.02 \text{ MHz}$ for $\text{CsCdF}_3:\text{Fe}^{3+}$. The corresponding variation $\Delta A_s = 5.25$

TABLE VI. Values of the equilibrium $\text{Fe}^{3+}\text{-F}^-$ distance, R_e , obtained for Fe^{3+} doped ANF_3 ($A = \text{K, Rb, Cs}$; $N = \text{Mg, Zn, Cd}$) fluoroperovskites from total-energy calculations on $\text{FeF}_6\text{A}_8\text{N}_6^{17+}$ clusters. Calculations have been performed using the ADF code, the local-density approximation (LDA) and including the Madelung potential due to the rest of the lattice. The results are compared to those derived from the analysis of the experimental isotropic superhyperfine constant, A_s , using Eqs. (2) and (6) and assuming $n = 6$ and a value $R_e = 193.3$ pm for $\text{KMgF}_3\text{:Fe}^{3+}$. The values of A_s taken from Table I are included. R_0 values are also included for comparison.

Host lattice	R_0 (pm)	A_s (MHz)	R_e (pm) (from A_s)	R_e (pm) (from total energy)
KMgF_3	1.987	71.23 ± 0.06	193.3	193.3
KZnF_3	2.027	70.3 ± 0.3	193.7 ± 0.2	196.6
RbCdF_3	2.200	66.1 ± 0.3	195.6 ± 0.2	197.4
CsCdF_3	2.232	65.98 ± 0.02	195.65 ± 0.03	198.6

± 0.08 MHz would be ascribed to an increase $\Delta R_e = 2.4$ pm assuming $n_s = 6$. For more confidence concerning this interpretation, the R_e value has also been calculated for Fe^{3+} -doped ANF_3 ($A = \text{K, Rb, Cs}$; $N = \text{Mg, Zn, Cd}$) fluoroperovskites by means of total-energy calculations on $\text{FeF}_6\text{A}_8\text{N}_6^{17+}$ clusters. The comparison between R_e values derived from these calculations and from the analysis of experimental A_s values is given on Table VI.

The substitution of a N^{2+} cation in the perfect ANF_3 lattice by an impurity leads to a change of the distance with the F^- which is reflected by the displacement $u = (R_e - R_0)$. From the results collected in Table VI it is found that $u/R_0 = -3\%$ for $\text{KMgF}_3\text{:Fe}^{3+}$ while it is equal about -10% for $\text{ACdF}_3\text{:Fe}^{3+}$ ($A = \text{Rb, Cs}$). As in the present calculations of R_e , no relaxation has been allowed to second and third neighbors the right metal-ligand distances should be *smaller* than the calculated ones, especially for $\text{ACdF}_3\text{:Fe}^{3+}$ ($A = \text{Rb, Cs}$) involving a higher $|u/R_0|$ value. Having in mind this fact and accepting an error of $\pm 1\%$ on the R_e values coming from total-energy calculations, the two sets of figures in Table VI can certainly be compatible. To achieve a better value of R_e for the whole series of fluoroperovskites doped with Fe^{3+} calculations on bigger clusters, allowing the relaxation of further ions in $\langle 100 \rangle$ directions are required. Work along this line is in progress.

From the present analysis R_e increases around $\Delta R_e = 2.4$ pm on passing from $\text{KMgF}_3\text{:Fe}^{3+}$ to $\text{CsCdF}_3\text{:Fe}^{3+}$ while $\Delta R_e = 7 \pm 1$ pm when Mn^{2+} is involved. The interaction of ligands of a complex such as FeF_6^{3-} or MnF_6^{4-} with further neighbors of the host lattice is responsible for the modifications of R_e when a host lattice is replaced by another one with a similar structure. On going from $\text{KMgF}_3\text{:Fe}^{3+}$ to $\text{CsCdF}_3\text{:Fe}^{3+}$ such an interaction leads to a variation of the chemical pressure on the MF_6 complex ($M = \text{Mn}^{2+}, \text{Fe}^{3+}$) which, in a first approximation, can be taken as independent of the nature of central cation.

Compared to $\hbar\omega(A_{1g}) = 540 \text{ cm}^{-1}$ found for FeF_6^{3-} , the value⁵⁵ for MnF_6^{4-} is clearly smaller [$\hbar\omega(A_{1g}) \approx 400 \text{ cm}^{-1}$] following the diminution of the nominal charge associated with the central cation.⁵⁰ From this simple argument it can thus be expected that on passing from $\text{KMgF}_3\text{:Mn}^{2+}$ to $\text{CsCdF}_3\text{:Mn}^{2+}$ the ΔR_e value will be about twice that corresponding to the Fe^{3+} impurity.

The strong R dependence of A_s is also partially reflected looking at the variations of A_s with temperature. For instance, $A_s = 64.2 \pm 1.1$ MHz for $\text{CsCdF}_3\text{:Fe}^{3+}$ at room temperature.³⁰ The diminution of 2 ± 1 MHz when compared to the ENDOR value (Table I) is consistent with thermal expansion effects. It is worthwhile to remark, however, that apart from this contribution to $(\partial A_s / \partial T)_P$ there is also the so-called explicit contribution given by $(\partial A_s / \partial T)_V$ which is not easy to evaluate *a priori*.^{56,57}

D. Dependence of $10Dq$ on the spin density f_s

Despite the smallness of f_s , it has been demonstrated for CrF_6^{3-} and MnF_6^{4-} units that the $10Dq$ value as well as its R dependence are strongly related to such a spin density. For showing the importance played by the small $3d\text{-}2s(F)$ hybridization in the present case $\text{MSX}\alpha$ and SCCEH calculations suppressing the $2s(F)$ orbitals from the basis set have also been carried out. Representative results are displayed in Table VII. In a normal calculation the obtained $10Dq$ values at $R = 190$ pm are comparable to the experimental one ($10Dq \approx 13\,300 \text{ cm}^{-1}$).⁵⁸ Moreover, writing in the vicinity of $R = 190$ pm

$$10Dq = AR^{-n} \quad (8)$$

the exponent n is found to be equal to 4.6 and 3.5 from SCCEH and $\text{MSX}\alpha$ calculations, respectively. This value indicates that $10Dq$ would also be a useful parameter for measuring variations of the metal-ligand distance for Fe^{3+} in fluorides such as it has been done^{8,9,41,59} in the case of Mn^{2+} , Ni^{2+} , or Cr^{3+} . Unfortunately little is known about optical excitations of Fe^{3+} impurities in cubic fluorides.

When the $2s(F)$ orbitals are removed from the basis set f_s is only slightly modified while the value of $10Dq$ decreases and its R dependence is substantially modified. This behavior (similar to that previously found for CrF_6^{3-} and MnF_6^{4-} units) stresses that the R dependence of $10Dq$ for FeF_6^{3-} is again related to that of the small transferred spin density f_s . This fact explains the microscopic origin of the R dependence of $10Dq$ pointing out the existence of a connection between an optical parameter such as $10Dq$ and an EPR parameter such as A_s . Why the suppression of the small $3d\text{-}2s(F)$ hybridization leads to the dramatic changes displayed in Table VII is explained in detail in Ref. 53.

TABLE VII. Calculated values of the crystal-field constant $10Dq$ (in cm^{-1}) and spin-density parameters, f_s and f_σ (in %), obtained through MS- $X\alpha$ (first row) and SCCEH (second row) methods for the FeF_6^{3-} cluster at different metal-ligand distances, R (in pm). The values of the exponent n corresponding to the fit of the parameters to the expression CR^{-n} (C =constant) are also given.

R	Normal Calculation			Calculation without $2s(F)$		
	$10Dq$	f_s	f_σ	$10Dq$	f_s	f_σ
185	16 370	1.74	7.87	10 043		10.68
	18 715	2.06	6.19	3080		7.64
190	14 730	1.39	8.40	9714		10.83
	16 560	1.74	6.44	3600		7.90
195	13 630	1.13	8.87	9305		10.96
	14 730	1.47	6.70	4014		8.16
n	3.48	8.20	-2.27	1.44		-0.49
	4.55	6.41	-1.50	-5.04		-0.21

IV. FINAL REMARKS

The present results demonstrate that variations of the distance between the Fe^{3+} impurity and F^- ligands can be well measured through experimental A_s and $10Dq$ parameters. These changes can be produced either by a hydrostatic pressure, by the substitution of the host lattice by another one with the same structure and also by a structural phase transition of the matrix.^{60,24}

Despite the metal-ligand distance for the perfect CsCdF_3 lattice (equal to $a/2$) is 23 pm higher than that corresponding to KMgF_3 such a difference becomes *only* about 2.5 pm when Fe^{3+} impurities replace the divalent host lattice cation according to the present interpretation of A_s data. This conclusion is also compatible with the R_e value derived from the present total-energy calculations. First analysis by Rubio *et al.* (Ref. 6) of the zero-field splitting parameter, b_4^0 , using the *empirical* superposition model, suggested a similar conclusion. These authors assumed, however, a value $R_e = 1.99$ pm for $\text{KMgF}_3:\text{Fe}^{3+}$ which is about 5 pm higher than that expected from the present work.

When changes of the $\text{Fe}^{3+}-\text{F}^-$ distance induced by an applied pressure are followed through A_s , the resolution would be about ± 0.5 pm using EPR measurements or ± 0.05 pm if the ENDOR technique were employed. These figures are to be compared with the EXAFS resolution which is ± 1 pm in the best case.¹⁻⁵

The calculated R_e values for Fe^{3+} -doped fluorides indicate that accurate DFT calculations on clusters including *only* up to third neighbors appear as a useful tool for knowing the *actual* impurity-ligand distance in insulating host lattices. The same conclusion was reached in the study of Cr^{3+} and Tl^{2+} impurities in halide lattices.^{18,17,61} It is worth noting that the electron trapping by a species T can depend strongly upon the local relaxation in the ground state of the T center formed *after* the electron capture. This happens, for instance, for $[\text{MC}_5(\text{NO})]^{2-}$ species⁶² ($M=\text{Os}, \text{Ru}$) in AgCl or for the Ag^+ impurity in KCl .⁶³ In the latter case the electronic stability of the Ag^0 center is found to require⁶³ a local outward relaxation higher than 8%. The analysis of the experimental A_s value suggests an outward relaxation close to 17%.

It is worthwhile to remark that not all the parameters are

equally reproduced by a *given* calculation. In the present case R_e values derived from the R dependence of the total energy are equal to the experimental ones within $\pm 1.5\%$. By contrast, the experimental A_s value at $R=191$ pm is not so well reproduced by the calculations. Despite this fact, all calculations lead practically to the same value of the n_s exponent, thus supporting that A_s variations can be used for measuring changes of the distance due to an applied pressure or a host-lattice change.

The knowledge of the true $\text{Fe}^{3+}-\text{F}^-$ distance is also relevant for determining the R dependence of other spectroscopic parameters. This is especially important in the case of EPR parameters such as b_4^0 , which can only be measured when Fe^{3+} enters a diamagnetic host lattice as a *diluted* impurity.⁶⁴⁻⁶⁶ From experimental data on b_4^0 for Fe^{3+} in fluoroperovskites it appears^{6,64} that b_4^0 does not depend only on R such as it occurs for A_s . Additional experimental work is, however, necessary for being sure on this conclusion.

Despite experimental A_s values corresponding to octahedral FeF_6^{3-} units (Table I) being all very close, a different situation comes out when the tetragonal FeOF_5^{4-} center^{67,68} is considered. For instance, ENDOR data for that center⁶⁵ in KMgF_3 give $A_s = 30.8 \pm 0.25$ MHz for the axial F^- ion, while for equatorial ones, A_s is essentially coincidental with the value for the FeF_6^{3-} center (Table I). Compared to figures gathered in Table I, the value $A_s = 31$ MHz, suggests that the distance between Fe^{3+} and the axial F^- ion is higher than 195 pm. The present study cannot, however, be directly applied to this center as the substitution of F^- by oxygen should lead to an important change of the electronic structure. Work along this direction is in progress.

The experimental results collected in Table V and those reached by means of DFT calculations indicate that R_e for $\text{KMgF}_3:\text{Fe}^{3+}$ would be about 3 pm higher than for Fe^{3+} in fluoroelpasolite lattices. This conclusion is, however, not clear regarding the A_s values of Table I and suggests that the value of the K factor in formula (6) changes slightly on passing from a type of lattice to another one. Microscopically this could reflect the different form of the electrostatic potential, V_R^{el} , due to the rest of the lattice in elpasolite and perovskite lattices. Preliminary results support this view.

The use of A_s for measuring R variations could also be applied to other Fe^{3+} centers and also to other TM impurities with unpaired σ electrons. For instance A_s has been measured in the case of tetrahedral FeCl_4^{1-} species formed inside NaCl or AgCl lattices.⁶⁹ In the case of II-VI semiconductors shf interaction has been detected for ZnSe doped with TM impurities.⁷⁰

Work along these lines is planned for the near future.

Note added in proof. Recent ADF calculations on clusters of 21 atoms around the Mn^{2+} impurity [J. Phys.: Condens. Matter **11**, L525 (1999)] reproduce the R_e values of Mn^{2+} -doped fluoroperovskites derived from experimental A_s and $10Dq$ parameters.

ACKNOWLEDGMENTS

Kind information on iron compounds by Professor J. L. Fourquet (University of Le Mans) and Professor A. Tressaud (University of Bordeaux) is acknowledged. This work has partially been supported by the CICYT under Project No. PB98-0190.

- ¹W. F. Pong, R. A. Mayanovic, B. A. Bunker, J. K. Furdyna, and U. Debska, *Phys. Rev. B* **41**, 8440 (1990).
- ²J. H. Barkyoumb and A. N. Mansour, *Phys. Rev. B* **46**, 8768 (1992).
- ³C. Zaldo, C. Prieto, H. Dexpert, and P. Fessler, *J. Phys.: Condens. Matter* **3**, 4135 (1991).
- ⁴M. C. Marco de Lucas, F. Rodríguez, C. Prieto, M. Verdaguer, M. Moreno, and H. U. Güdel, *Radiat. Eff. Defects Solids* **135**, 95 (1995).
- ⁵T. Murata, S. Emura, H. Ito, and H. Maeda, *Physica B* **158**, 613 (1989).
- ⁶J. Rubio, H. Murrieta, and G. Aguilar, *J. Chem. Phys.* **71**, 4112 (1979).
- ⁷M. T. Barriuso and M. Moreno, *Phys. Rev. B* **29**, 3623 (1984), and references therein.
- ⁸F. Rodríguez and M. Moreno, *J. Chem. Phys.* **84**, 692 (1986).
- ⁹B. Villacampa, R. Cases, V. M. Orera, and R. Alcalá, *J. Phys. Chem. Solids* **55**, 263 (1994).
- ¹⁰C. Marco de Lucas, F. Rodríguez, and M. Moreno, *Phys. Rev. B* **50**, 2760 (1994).
- ¹¹B. Villacampa, R. Alcalá, P. J. Alonso, M. Moreno, M. T. Barriuso, and J. A. Aramburu, *Phys. Rev. B* **49**, 1039 (1994).
- ¹²Dong-Ping Ma and D. E. Ellis, *J. Lumin.* **71**, 329 (1997).
- ¹³M. Flórez, M. A. Blanco, V. Luña, and L. Pueyo, *Phys. Rev. B* **49**, 69 (1994).
- ¹⁴A. M. Woods, R. S. Sinkovits, J. C. Charpie, W. L. Huang, R. H. Bartram, and A. R. Rossi, *J. Phys. Chem. Solids* **54**, 543 (1993).
- ¹⁵D. J. Groh, R. Pandey, and J. M. Recio, *Phys. Rev. B* **50**, 14 860 (1994).
- ¹⁶J. L. Pascual, L. Seijo, and Z. Barandiarán, *Phys. Rev. B* **53**, 1 (1996).
- ¹⁷F. Gilardoni, J. Weber, K. Bellafrouth, C. Daul, and H. U. Güdel, *J. Chem. Phys.* **104**, 7624 (1996).
- ¹⁸J. A. Aramburu, M. Moreno, K. Doclo, C. Daul, and M. T. Barriuso, *J. Chem. Phys.* **110**, 1497 (1999).
- ¹⁹A. Leblé, Thèse d'Etat, Université du Maine, 1982.
- ²⁰G. Blasse and B. C. Grabmaier, *Luminescent Materials* (Springer-Verlag, Berlin, 1994), p. 50.
- ²¹A. Poirier and D. Walsh, *J. Phys. C* **16**, 2624 (1983).
- ²²B. A. Wilson, W. M. Yen, J. Hegarty, and G. F. Imbusch, *Phys. Rev. B* **19**, 4238 (1979).
- ²³L. Helmholz, *J. Chem. Phys.* **32**, 302 (1960).
- ²⁴J. M. Dance, J. Grannec, A. Tressaud, and M. Moreno, *Phys. Status Solidi B* **173**, 579 (1992).
- ²⁵R. C. DuVarney, J. R. Niklas, and J. M. Spaeth, *Phys. Status Solidi B* **103**, 329 (1981).
- ²⁶R. K. Jeck and J. J. Krebs, *Phys. Rev. B* **5**, 1677 (1972).
- ²⁷T. P. P. Hall, W. Hayes, R. W. H. Stevenson, and J. Wilkens, *J. Chem. Phys.* **38**, 1977 (1963).
- ²⁸P. Studzinski and J. M. Spaeth, *J. Phys. C* **19**, 6441 (1986).
- ²⁹C. D. Adam, J. Owen, and M. E. Ziaei, *J. Phys. C* **11**, L117 (1978).
- ³⁰J. J. Rousseau, M. Rousseau, and J. C. Fayet, *Phys. Status Solidi B* **73**, 625 (1976).
- ³¹H. Levanon, G. Stein, and Z. Luz, *J. Chem. Phys.* **53**, 876 (1970).
- ³²J. Emery and J. C. Fayet, *Solid State Commun.* **42**, 683 (1982).
- ³³G. Te Velde and E. J. Baerends, *J. Comput. Phys.* **99**, 84 (1992).
- ³⁴P. Belanzoni, E. J. Baerends, S. van Asselt, and P. B. Langewen, *J. Phys. Chem.* **99**, 13 094 (1995).
- ³⁵H. Bode and E. Voss, *Z. Anorg. Allg. Chem.* **290**, 1 (1957).
- ³⁶M. Leblanc, J. Panneteir, G. Ferey, and R. De Pape, *Rev. Chim. Miner.* **22**, 107 (1985).
- ³⁷J. L. Fourquet, E. Courant, P. Chevalier, and R. De Pape, *Acta Crystallogr., Sect. C: Cryst. Struct. Commun.* **41**, 165 (1985).
- ³⁸J. L. Fourquet and H. Duroy, *J. Solid State Chem.* **103**, 353 (1993).
- ³⁹D. Babel, *Struct. Bonding (Berlin)* **3**, 1 (1968).
- ⁴⁰S. Sugano and R. G. Shulman, *Phys. Rev.* **130**, 517 (1963).
- ⁴¹M. C. Marco de Lucas, J. M. Dance, F. Rodríguez, A. Tressaud, M. Moreno, and J. Grannec, *Radiat. Eff. Defects Solids* **135**, 19 (1995).
- ⁴²K. Wissing, J. A. Aramburu, M. T. Barriuso, and M. Moreno, *Solid State Commun.* **108**, 1001 (1998); *J. Chem. Phys.* **111**, 10 217 (1999).
- ⁴³S. H. Vosko, L. Wilk, and M. Nusair, *Can. J. Phys.* **58**, 1200 (1980).
- ⁴⁴A. D. Becke, *Phys. Rev. A* **38**, 3098 (1988); J. P. Perdew, *Phys. Rev. B* **33**, 8822 (1986).
- ⁴⁵S. Sugano, Y. Tanabe, and H. Kamimura, *Multiplets of Transition-Metal Ions in Crystals* (Academic Press, New York, 1970).
- ⁴⁶R. G. Parr and W. Yang, *Density-Functional Theory of Atoms and Molecules* (Oxford, New York, 1989), p. 141.
- ⁴⁷J. A. Aramburu, M. Moreno, and M. T. Barriuso, *J. Phys.: Condens. Matter* **4**, 9089 (1992).
- ⁴⁸A. Tressaud, Thèse Université de Bordeaux, 1969; (private communication).
- ⁴⁹A. Tressaud, J. Portier, R. de Pape, and P. Hagenmuller, *J. Solid State Chem.* **2**, 269 (1970).
- ⁵⁰K. Nakamoto, *Infrared and Raman Spectra of Inorganic and Coordination Compounds*, 4th ed. (Wiley, New York, 1986).
- ⁵¹M. Couzi, S. Khairoun, and A. Tressaud, *Phys. Status Solidi A* **98**, 423 (1986).
- ⁵²K. Wieghardt and H. H. Eysel, *Z. Naturforsch. B* **25**, 105 (1970).
- ⁵³M. Moreno J. A. Aramburu, and M. T. Barriuso *Phys. Rev. B* **56**, 14 423 (1997); M. Moreno, M. T. Barriuso, and J. A. Aramburu, *Int. J. Quantum Chem.* **52**, 829 (1994).
- ⁵⁴R. P. Messmer and G. D. Watkins, *Phys. Rev. B* **7**, 2568 (1973).
- ⁵⁵M. Marco de Lucas, F. Rodríguez, and M. Moreno, *J. Phys.: Condens. Matter* **7**, 7535 (1995).
- ⁵⁶W. M. Walsh, J. Jeener, and N. Bloembergen, *Phys. Rev.* **139**, A1338 (1965).
- ⁵⁷F. Rodríguez, M. Moreno, J. M. Dance, and A. Tressaud, *Solid State Commun.* **69**, 67 (1989).
- ⁵⁸A. B. P. Lever, *Inorganic Electronic Spectroscopy* (Elsevier, Amsterdam, 1984), p. 741.
- ⁵⁹S. J. Duclos, Y. K. Vohra, and A. L. Ruoff, *Phys. Rev. B* **41**, 5372 (1990).
- ⁶⁰I. Flerov, M. Gorev, K. Aleksandrov, A. Tressaud, J. Grannec, and M. Couzi, *Mat. Sci. Eng., R.* **24**, 81 (1998).
- ⁶¹I. Cabria, M. Moreno, J. A. Aramburu, M. T. Barriuso, U. Rogulis, and J. M. Spaeth, *J. Phys.: Condens. Matter* **10**, 6481 (1998).
- ⁶²R. S. Eachus, R. C. Baetzold, Th. Pawlik, O. Poluektov, and J. Schmidt, *Phys. Rev. B* **59**, 8560 (1999).
- ⁶³I. Cabria, M. T. Barriuso, J. A. Aramburu, and M. Moreno, *Int. J. Quantum Chem.* **61**, 627 (1997).
- ⁶⁴Y. Wan-Lun and C. Rudowicz, *Phys. Rev. B* **45**, 9736 (1992).
- ⁶⁵Z. Wen-Chen, *J. Phys. Chem. Solids* **55**, 433 (1994).
- ⁶⁶Y. Wan-Lun, *Phys. Rev. B* **52**, 4237 (1995).

⁶⁷D. C. Stjern, R. C. DuVarney, and W. P. Unruh, *Phys. Rev. B* **10**, 1044 (1974).

⁶⁸J. Y. Buzare and J. C. Fayet, *Solid State Commun.* **21**, 1097 (1977).

⁶⁹S. V. Nistor, Th. Pawlik, and J. M. Spaeth, *J. Phys.: Condens. Matter* **7**, 2225 (1995).

⁷⁰J. Dziesiaty, P. Peka, M. U. Lehr, H. J. Schulz, and A. Klimakow, *Phys. Rev. B* **49**, 17 011 (1994).